ADVANCED ELECTRONIC MATERIALS
www.advelectronicmat.de

Single-Molecule Doping: Conductance Changed By Transition Metal Centers in Salen Molecules

*Filip Kilibarda, Alexander Strobel, Torsten Sendler, Matthias Wieser, Michael Mortensen, Julie Brender Trads, Manfred Helm, Jochen Kerbusch, Elke Scheer, Sibylle Gemming, Kurt V. Gothelf, and Artur Erbe**

The creation of molecular components for use as electronic devices has made enormous progress. In order to advance the field further toward realistic electronic concepts, methods for the controlled modification of the conducting properties of the molecules contacted by metallic electrodes need to be further developed. Here a comprehensive study of charge transport in a class of molecules that allows modifications by introducing metal centers into organic structures is presented. Single molecules are electrically contacted and characterized in order to understand the role of the metal centers in the conductance mechanism through the molecular junctions. It is shown that the presence of single metal ions modifies the energy levels and the coupling of the molecules to the electrical contacts, and that these modifications lead to systematic variations in the statistical behavior of transport properties of the molecular junctions. A rigorous statistical analysis of thousands of junctions is performed to reveal this correlation. The understanding of the role of the metal ion in the resulting conductance properties is an essential step toward the development of molecular electronic circuits.

1. Introduction

The great success of semiconducting materials in building today's electronics relies mostly on the possibility to control the conductivity of the materials by modifying their composition. Any new technology that is developed as an alternative for semiconductor-based nanoelectronics must provide equivalent or superior control mechanisms. The field of molecular electronics has progressed in recent years and demonstrated functionalities such as single-molecule switches,[1,2] field emitters,[3] and even gateable structures.[4,5] Variations of the overall conductance of all these structures in nominally identical junctions were, however, large. Differences in conductance between these junctions were identified by recording conductance histograms of all measured junctions. Large conductance variations could be demonstrated between high- and low-conductance states by using quantum interference effects[5] or by changing the molecular structures in a controlled way.[6] To be able to use molecules as future components in electronic applications, it would be useful not only to have binary, high and low, conductance states available, but also a range of possible modifications to fine-tune the exact properties of the circuit. Metallorganic components lend themselves for this purpose because of the broad palette of ions, promising also a broad range of achievable conductance properties. The influence of metal ions incorporated into porphyrin molecules has already been investigated, showing a decrease in conductance due to destabilization of the π-system by metal

F. Kilibarda, A. Strobel, T. Sendler, M. Wieser, M. Helm, J. Kerbusch, A. Erbe
Helmholtz-Zentrum Dresden-Rossendorf
Bautzner Landstraße 400
Dresden 01328, Germany
E-mail: a.erbe@hzdr.de

M. Helm, J. Kerbusch, S. Gemming, A. Erbe
Center for Advancing Electronics Dresden
Technische Universität Dresden
Dresden 01062, Germany

The ORCID identification number(s) for the author(s) of this article can be found under https://doi.org/10.1002/aelm.202100252.

DOI: 10.1002/aelm.202100252

M. Mortensen, J. B. Trads, K. V. Gothelf
Department of Chemistry and Interdisciplinary Nanoscience Center
Centre for DNA Nanotechnology
iNANO
Gustav Wieds Vej 14, Aarhus C 8000, Denmark

E. Scheer
Department of Physics
University of Konstanz
Konstanz 78457, Germany

S. Gemming
Institute of Physics
Technische Universität Chemnitz
Chemnitz 09107, Germany

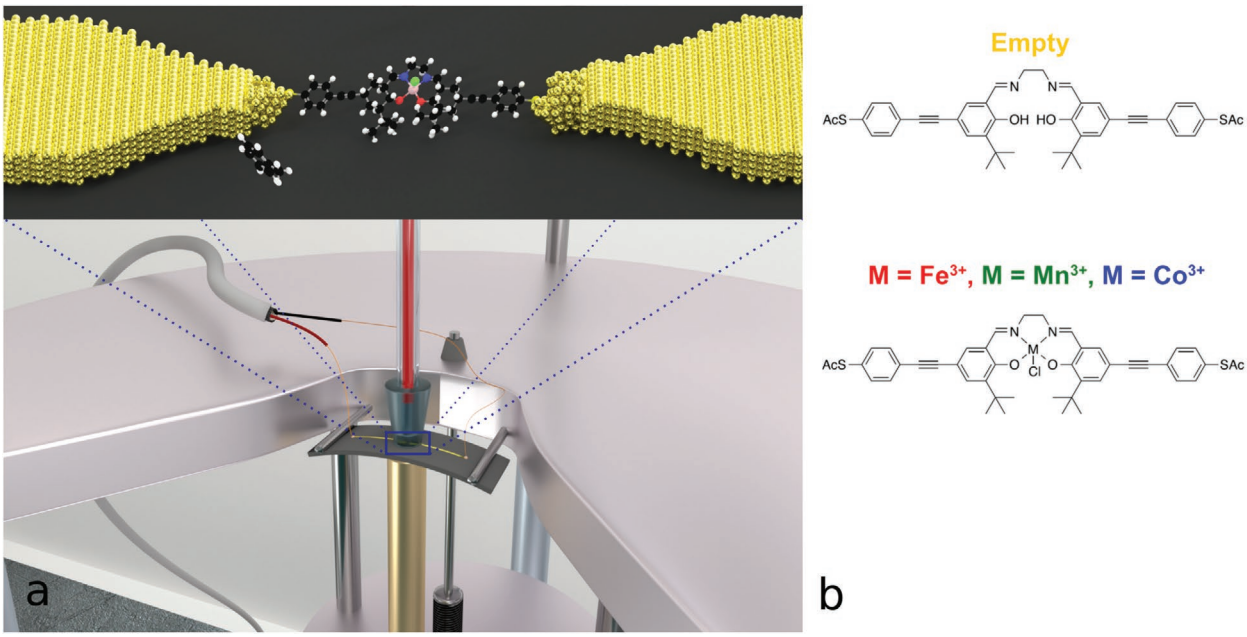

Figure 1. Salen molecules in break junctions. a) The salen molecule is anchored, via thiol terminal groups (yellow) at each end, between two Au electrodes formed in a mechanically controllable break junction. b) For the Empty molecule, the π-system of the delocalized electrons is broken in the center of the ligand. This leads to a tunneling barrier, which is eliminated by integrating a Fe^{3+}, Mn^{3+} or Co^{3+} transition metal ion.

complexation[7] and a sigma character of the metal-carbon bonds.[8] Studies on in situ metal doped nitrilotriacetic acid complexes showed a decrease in conductance due to the increased length of the metal doped molecules.[9] Conductance trends more related to the binding energy than to the metal dopands are seen in bis-2,2′:6′,2″-terpyridin complexes.[10] Devices containing such molecular complexes were demonstrated to act as single-molecular transistors based on Coulomb interaction[11,12] and on redox reactions.[13,14] Instead of conformational changes, the use of different metal ions with multiple valence states would allow for a far better control of the properties and a much wider range of possible conductance adjustments.

Here, we present studies of the conductance of single-molecule junctions of salen complexes composed of a salen ligand containing two 4-acetylthiophenylacetylene moieties, a transition metal ion M (Fe^{3+}, Mn^{3+} or Co^{3+}) (**Figure 1**), and an axial chloride ligand.[15–17] Only one chloride ion is associated with the metal-salen complexes. The excessive chloride ions from the preparation are removed in the workup procedure during the synthesis of the complexes as described in the Supporting Information. For all three complexes the Salen-M(III)Cl complexes are air stable and can be handled without special precautions which is the main reason for using this oxidation state and the use of chloride as the counterion. The molecule is designed to anchor to gold electrodes by formation of Au-S bonds after in situ removal of the acetyl protecting groups.[16] Compound Empty was prepared from the respective salicylaldehydes and subsequently the metal ions were inserted (see Supporting Information). The transition metal center preferably coordinates in-plane to the N and O atoms of the salen ligand and axially to the chloride ligand.

Salen is composed of two fully conjugated, rigid planar halves, which are linked by a flexible, non-conducting aliphatic bridge. The metal ion forms two coordinative bonds with each of the two halves. The exact mechanism has not yet been treated theoretically but the coordination of two conjugated π systems by a metal ion is expected to increase the coupling between these two parts since the orbitals of the conjugated system can interact with the orbitals at the metal. This idea is fundamentally different from the case of porphyrin molecules, where a conjugated system exists even without the metal ion,[7,18] and of terpyridine-based complexes, in which the metal ions act as tunnel barriers in the absence of chemical gating.[10] Coupling between two independent molecules via various metal ions has been demonstrated.[19] Studies of transistors based on salen crystals containing various metal ions exhibit strong effects of the molecular conformation on the stacking of the crystals, which in turn influence the conductivity of the materials.[20]

The role of the metal centers is elucidated by recording conductance histograms in conventional stretching curves and, in addition, thousands of $I(V)$ curves at various states of the opening and closing of the single-molecule junctions. We show that the combined information extracted from both characterization methods leads to a consistent picture of the variations induced by the different metal centers.

2. Results and Discussion

The conductance values of the molecular components in the linear regime[21] are investigated by using histograms of stretching curves (**Figure 2**).

Before breaking the nanojunctions completely, we observe conductance plateaus at 1 G_0 ($G_0 = 2e^2/h$), the quantum of

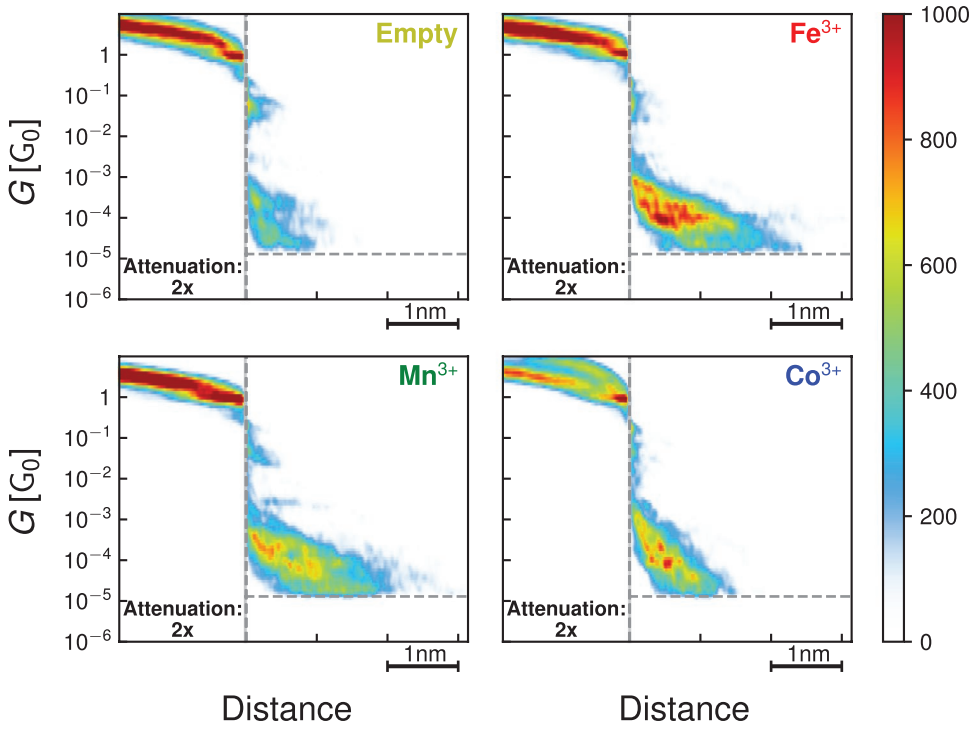

Figure 2. Histograms of stretching curves: Measurements on all compounds exhibit a plateau at the quantum of conductance G_0, showing that a clean, single-atom Au contact is formed prior to breaking (step-wise behavior in the gray segments of the histograms). Original bin values in the area left of the vertical dashed line are attenuated by the factor of two for better representation, that is, the intensity scale maximum in the gray area is 2000 counts. The vertical line represents the last occurrence of the G_0 value, while the horizontal line represents the end-point for contact stretching ($R_{lim} = 10^9\,\Omega$). It is important to state that this is not the limiting factor of the measurement device but rather a range of interest for the given molecule. At lower conductance values, Fe^{3+}, Mn^{3+}, and Co^{3+} show conductance plateaus between 1×10^{-3} and 1×10^{-5} G_0 in 30 % to 40 % of all curves. In this range, Empty shows only a small number of measurement points. The plateau found in the measurements on Co^{3+} is shorter and more tilted compared to plateaus for Mn^{3+} and Fe^{3+}. (Empty: 200 curves, Fe^{3+}: 203 curves, Mn^{3+}: 200 curves, Co^{3+}: 189 curves)

conductance, for all compounds, indicating a clean single-atom Au contact,[22] followed by a strong decay of conductance immediately after breaking the contact. When reaching a conductance value of 1×10^{-5} G_0 the bridge is closed again to 20 G_0 to make sure a clean Au tip is formed in the subsequent opening. We therefore show a dashed line at $G = 1 \times 10^{-5}$ G_0 in the histograms in Figure 2, to indicate that conductance values below this point were not recorded.

Due to the tunneling barrier in the ethylene diamine center of the non-coordinated salen molecule, Empty exhibits only very short conductance plateaus, which may be related to direct tunneling as well. The weak background signal at distances below 2 Å arises mainly from direct tunneling through toluene[23] or non-resonant tunneling through the molecule. We therefore conclude from the characterization of the Empty molecule that conductance without the presence of the metal ions cannot be distinguished from the conductance through the solvent in the stretching curves.

In contrast to this behavior, Fe^{3+}, Mn^{3+}, and Co^{3+} exhibit characteristic tilted plateaus in the range between 1×10^{-5} and 2×10^{-3} G_0 and in a length range between 1 and 2 nm. Thus, the conducting range extends far beyond the tunneling range, indicating that stable junctions with conducting molecules are formed. The pronounced tilt of the plateaus is a common feature of junctions with molecules that are longer than 2 nm.[24] The length of the conductance plateaus is in the range of 1 nm for both Fe^{3+} and Mn^{3+}, while the length is shorter (approximately 7 Å) for Co^{3+}. Here, we use the full set of recorded plateaus without data selection.

The stretching curves mostly show differences in the formation probability of the junctions at fixed bias voltage depending on the electrode distance. They seem to indicate only minor differences in the magnitude of the current. This may be caused by the applied voltage, which is in the linear range of charge transport through the molecular junction. The characteristics of the formed contacts can be very different, for example due to the electrode shape, the binding position of the molecule on the electrodes and steric effects of the molecule. Therefore measurement and analysis of $I(V)$s, recorded at various fixed positions during the stretching traces give additional insight into the nonlinear transport properties of the single-molecule junctions. For the analysis of the obtained data we use a simple transport model which assumes elastic transport through a single molecular level (SLM) and thus a single transport channel to describe the charge transport in the molecular junction.[25,26] We extract the energy E_0 of the level that carries the charge, the Lorentzian broadening Γ of this level due to the coupling with the metallic states in the leads, and the symmetry of the $I(V)$s, $\alpha = \frac{\Gamma_>}{\Gamma_<}$; $\Gamma_{>,<}$ is the larger and smaller value of the coupling parameters to the left (Γ_L) and to the right (Γ_R) electrode, respectively. The coupling parameter $\Gamma = \Gamma_L + \Gamma_R$

describes the electronic interaction between the molecule and the electrodes, which results in a broadening of the molecular level. The transmission T is then given by:[27]

$$T = \frac{4\Gamma_L\Gamma_R}{(E-E_0)^2+(\Gamma_L+\Gamma_R)^2} \quad (1)$$

The evaluation of the conductance states shows that a large majority of the curves cannot be fitted with the SLM describing elastic transport through a single channel (depending on the compound, only ≈2–8% can be well explained by the SLM). The main reasons for the reduced number of fitted curves are either junctions in which no molecules connect to both electrodes or molecular junctions which cannot be described by the SLM. Effects, which are not included in the SLM, are, for example, inelastic effects, Coulomb Blockade, contribution of multiple channels or resonances with non-Lorentzian shape. Thus, the use of the SLM is inappropriate for these junctions, although they are single-molecule junctions. While no filtering for the stretching curves was applied and therefore all physical transport regimes are displayed, the evaluation of $I(V)$ characteristics is applied only for contacts fulfilling the criteria of the SLM. Figure S18, Supporting Information, shows a time-series of all curves, which could be fitted for Fe in one of the samples. This series shows that the $I(V)$s which match the SLM were statistically distributed throughout the measurements and do not originate from a single event.

In order to quantify the appropriateness of the SLM for the junction, we calculate the goodness-of-fit (GOF) for each fit by using the adjusted R-square test:

$$R^2_{\text{adj}} = 1 - \frac{n-1}{n+p}\frac{\sum_i (y_i - f(x_i))^2}{\sum_i (y_i - \overline{y})^2} \quad (2)$$

Here, $f(x_i)$ and $\overline{y}$ are the fitted values and the mean of the measurement points, respectively, and n and p are the number of points and the number of degrees of freedom (in our case $n = 800$ and $p = 3$). In other words, R^2_{adj} shows how successful the model is at explaining the variation of the data. Generally, values span the range between 0 and 1 (negative values are also possible in the case of noise dominated datasets), where values of 1 represent perfect fits to the model.

To further validate the parameters obtained from the fitting of the $I(V)$ data, a wide range of initial conditions was used as a starting point in the fitting algorithm. Due to the unknown substructure of the hypersurface on which we search our solutions in the process of differential error minimization, it is possible that there are local solutions (local minima on the surface) which do not represent the best possible fit. Our algorithm can get stuck in these minima and would not truly determine the best solution. To rule out this possibility, we have chosen variation of the initial values even beyond the range of physically reasonable values. We have attempted fits starting with values which were 100 times smaller than the fit results to values which were 100 times larger. Our initial values were 0.5, 0.005, and 0.005 eV for E_0, Γ_L and Γ_R accordingly. A plot illustrating this search in the parameter space is given in the Supporting Information. From these calculations we conclude that for the curves with high GOF (GOF > 0.99), the starting values can be varied up to a factor of 10 times smaller or larger without changes in the solution.

The main conclusions drawn in this work are thus based on the curves that are modeled with a very high probability by the SLM, that is, for $R^2_{\text{adj}} > 0.99$ ($R^2_{\text{adj}} > 0.998$ for curves with high transmission, see below for definition). With this selection, we evaluate 474, 347, 557, and 865 curves for Empty, Fe, Mn, and Co compounds, respectively. In Figures S3– S8, Supporting Information, we also show comparisons of these results with the results obtained when including fits that show lower values of R^2_{adj}.

The development of Γ as a function of the total transmission for all four compounds is similar at first sight. All measurements exhibit two branches, which are separated into a low-conductance and a high-conductance part. Both parts show a quadratic dependence of Γ on T, which naturally arises from the relation of the two quantities for weak variation of E_0.[27]

The fact that similar behavior is found for all four compounds may be explained by the impact of the anchoring groups on the charge transport. The presence of two separate branches (**Figure 3**) may indicate two different binding geometries of the molecules on the metal electrodes. Thiol anchoring groups can lead to binding in three separate positions (atop, bridge, hollow) on the Au electrodes, leading to different conductance values of the resulting junctions.[28,29] Attribution of these positions to the branches found in the histograms cannot be deduced from the electrical characterization. Transmission values $T > 0.1$ lead, however, to $I(V)$ curves deviating only slightly from linear behavior. Therefore the curves in this transmission regime may be dominated by direct tunneling between the two metal electrodes. This could explain the presence of this branch in all four compounds.

The lower branch of the Γ vs. T curves exhibits clear differences between the four compounds. Co and Fe show a smooth increase of Γ toward a value of 0.05 eV at $T = 4 \times 10^{-3}$. This behavior is similar to that of the Empty molecule, which, however, shows a larger number of contacts toward higher transmission values of the lower branch, while the main number of curves for the Co and Fe compounds is found uniformly distributed. In combination with the observation of short plateaus in the stretching curves for the Empty molecule, the high transmission may indicate that direct tunneling between the metallic electrodes may be dominating for the Empty molecule, in line with the expectation that the Empty molecule basically acts as a tunnel barrier because the conjugation of the ligand is broken at the center of the molecule. The distribution of Γ values is different for the Mn compound. Here a stronger rise of the lower conductance branch toward values above 0.1 eV is seen. In addition, most of the points are accumulated at transmission values around 10^{-5}.

To fully understand the tuning of the molecular energy levels induced by the transition metal centers, we discuss now the role of the molecular level E_0, by taking a closer inspection of the energy versus transmission histograms (**Figure 4**). In the plot we see 2D histograms of the E_0 values extracted from $I(V)$ data for different compounds. States contributing to values around 0.6 eV are mainly found at transmissions around $T = 1 \times 10^{-3}$ for the Empty compound, and are equally

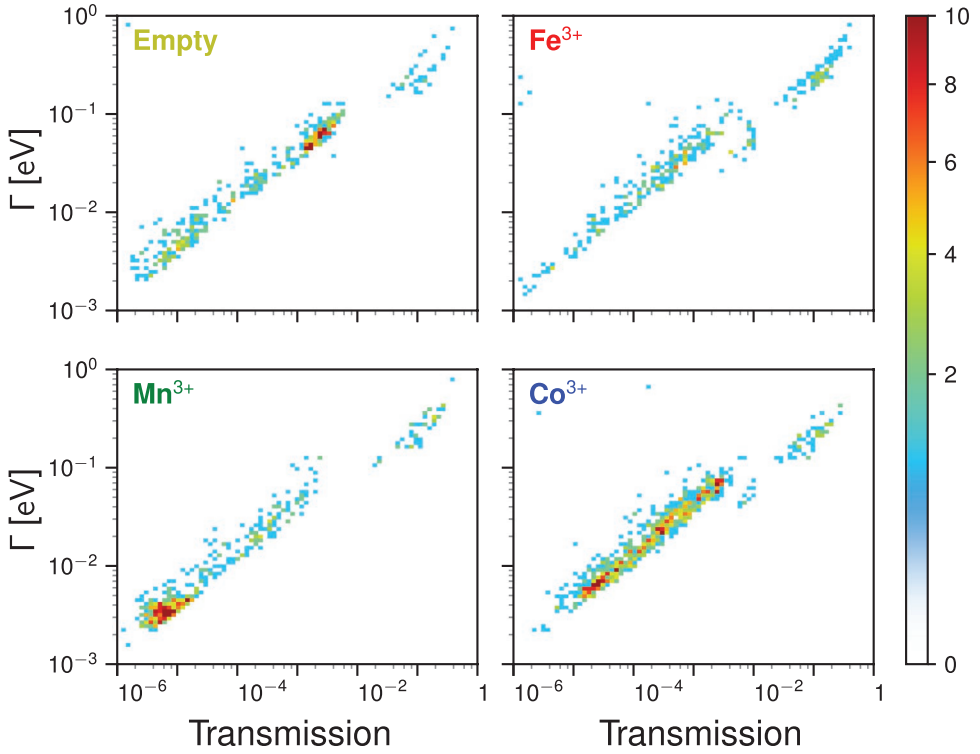

Figure 3. Histograms of the coupling values Γ: Obtained coupling values for all four compounds are plotted on log-log scale against the transmission values. The histograms show similar features, more precisely, the presence of two different coupling branches.

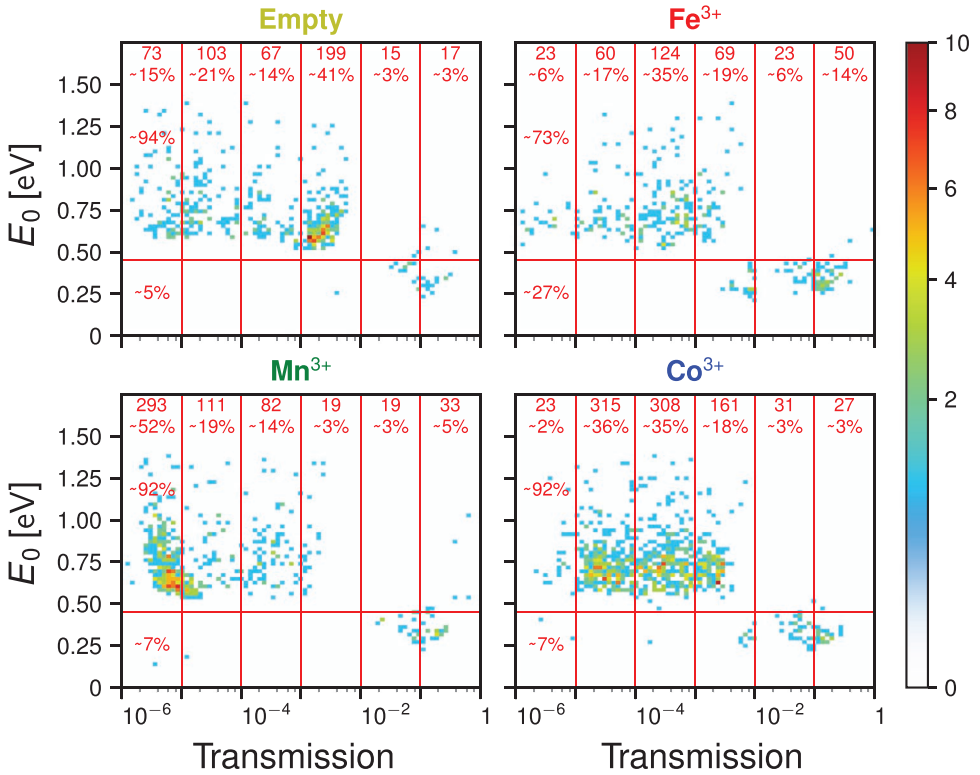

Figure 4. Histograms of the molecular level E_0: The occurrence of fit parameters for each value of E_0. Amount of curves that satisfy *GOF* > 0.99 for curves with transmission smaller than 0.01 and *GOF* > 0.998 for curves with transmission larger than 0.01 for each compound: Empty = 474, Fe^{3+} = 347, Mn^{3+} = 557, Co^{3+} = 865. (Total number of curves for each compound: Empty = 6716, Fe^{3+} = 19 094, Mn^{3+} = 12 426, Co^{3+} = 11 426)

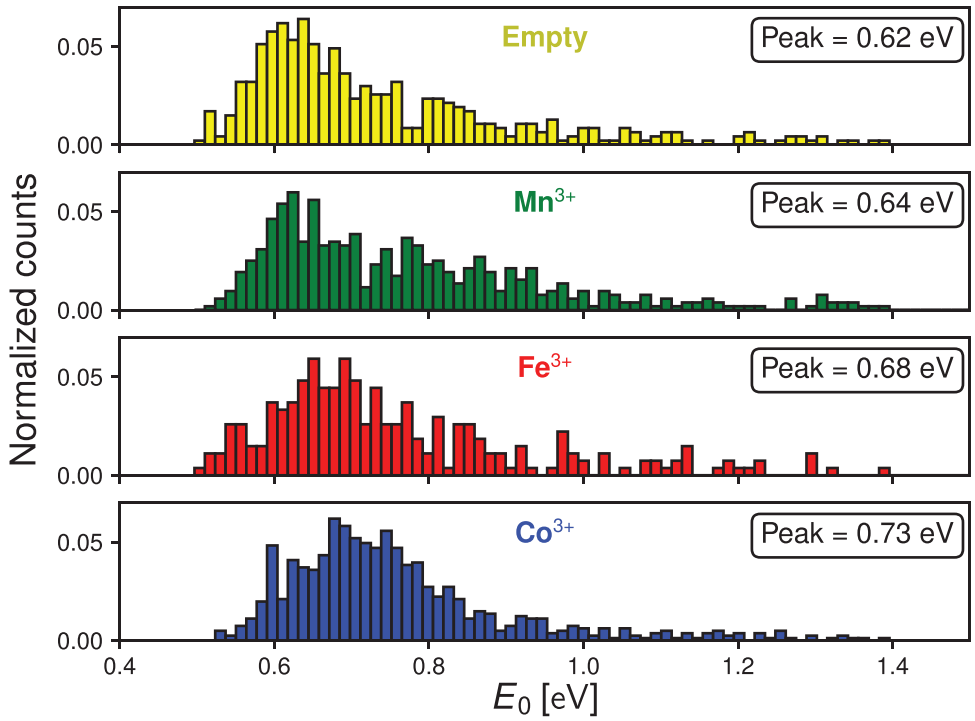

Figure 5. Comparison of energy levels E_0 for different ions: Estimated peaks represent the most probable value of E_0 for each compound. Different fitting functions were tried in obtaining the distribution fit, but none of them matched the obtained data perfectly (More details in Supporting Information) (Co^{3+}: 794 data points, Fe^{3+}: 252 data points, Mn^{3+}: 507 data points, Empty: 444 data points)

distributed in a range from 1×10^{-6} to 1×10^{-3} for the Fe and Co compound, supporting the interpretation that transport through the Empty molecule is limited by tunneling through the intermolecular barrier. As shown in ref. [23], tunnel contacts through solvents can be fitted by the SLM, but only in a narrow voltage and parameter range, in which the $I(V)$ curves only slightly deviate from linear behavior. For single-molecule junctions, in contrast, variations in coupling to the electrodes lead to changes of the parameters E_0 and Γ, which therefore can be distributed over a larger range. We find accumulations of fitted curves in transmission ranges from 10^{-5} to 10^{-3} for Fe and Co, which corresponds to the conductance plateaus found in the stretching curves, in particular when rejecting fits with GOF <0.99. When releasing the GOF criterion, we also find curves outside the range of the conductance plateaus in the stretching curves, see Figures S3, S4, S6, and S8, Supporting Information. Still, it is worth noting that the percentage of successful fits for the Fe compound is lower compared to the other compounds, which are represented by more diffuse point clouds. Therefore the behaviors of the Co compound and of the Fe compound are similar in terms of participating energies, but different in terms of statistical importance of these states. Just as the other compounds, the Mn compound shows two clouds of data points at similar energy values. A large portion of curves, however, show low transmission, around $T = 1 \times 10^{-5}$, indicating that $I(V)$s measured on the Mn compound can be fitted to the SLM for low coupling to the electrodes only, in agreement with the observation that the conductance plateaus extend to values below 10^{-5} G_0 for Mn.

The comparison between 2D conductance histograms and the $I(V)$ analysis shows that not all junctions that are formed can be described with the SLM. These might nevertheless be single-molecule junctions, but in which not all the assumptions of the SLM are fulfilled. The main assumptions are that one channel carries the charge transport through the junction and that the transmission through this channel can be approximated by a Lorentzian.

By accumulating the values of E_0 for different transmission values and plotting the upper branch of the data (values higher than 0.5 eV), we produce 1D histograms (**Figure 5**). This representation makes the differences between the compounds even more apparent, as we clearly observe the shifts of the energy levels. Peaks for the Empty compound are at 0.62 eV, for Mn at 0.64 eV. We further see higher values for the other two compounds, around 0.68 eV for Fe and 0.73 eV for Co.

3. Conclusion

To conclude, we state that incorporating metal ions into single-molecule junctions leads to changes in their charge transport characteristics. We have demonstrated the tuning of conductance of single-molecule junctions by varying the transition metal centers (Fe, Mn, Co) in salen ligands. The results achieved from stretching experiments were compared to those obtained from $I(V)$ characteristics of such contacts. It is one of our main conclusions that the full statistical evaluation including stretching and $I(V)$ curves of the junctions formed on a molecular species can lead to understanding their electrical

properties. A detailed analysis by means of the single-level transport model allowed mapping the energy landscape of the current-carrying channel in different salen complexes. Combining the information from the stretching curves and the analysis of the $I(V)$ characteristics indicates that different transport mechanisms dominate for molecules with different metal ions. In the Empty compound, tunneling seems to prevail, the Mn compound exhibits a large number of single-channel junctions in the range of the conductance plateau, while in the Fe molecule multiple channels or interactions seem to contribute. The formation of stable, tunable single-molecule contacts adds an important ingredient to the molecular toolbox. The use of salen complexes in the construction of branched conjugated nanostructures with the help of DNA-programmed assembly has been demonstrated in previous work.[30] In combination with the tunability demonstrated in the current work, this provides a major step toward the development of self-assembled integrated electronic circuits.

4. Experimental Section

Formation of Molecular Junctions: Metal salen complexes were prepared according to a protocol by Gothelf and co-workers for closely related metal salen complexes[15] (Supporting Information). The molecules, either Empty or already containing the metal ions, were solved in toluene, because this solvent showed low tunneling current and a marginal amount of curves which can be fitted to the SLM.[23] The influence of the solvent on energy values was low, as shown in previous experiments.[1] It could, however, be large on the distance dependence of the molecular conductance due to changes in the work function of the contacting metal.[31,32] Since it was intended to investigate the relative changes which were introduced by the presence of different ions into the salen molecules, all measurements were performed in toluene. The original complexes were immobilized on gold electrodes and their electronic properties were tested.[16] Thiol end-groups formed reliable junctions to gold nanoelectrodes[33,34] that were created in the mechanically controllable break junction (MCBJ) setup by breaking suspended Au nanowires on flexible polyimide substrates.[25] The molecules were dissolved in toluene with a droplet of aqueous ammonia to remove the acetyl protective groups. The toluene phase was separated and brought onto the samples in a liquid cell, which was further placed on top of the junction. Measurement in solution prevents degradation of the molecules, and increases the mobility of the molecules, to assure statistical sampling of many different molecules.

Electrical Characterization: For a comprehensive electrical characterization of junctions containing single molecules we performed and analyzed two sets of experiments. In the first set, we recorded the conductance of the junction during stretching and breaking the Au contact under a bias voltage of 100 mV and a very slow, constant bending speed (tip distance change in the order of 0.1 $Å s^{-1}$). Those so-called stretching curves contain information about the linear transport regime of the salen junction. The measured data were summarized in histograms by plotting the conductance against the relative displacement of the gold electrodes, which we obtained from the exponential decay of the current between the electrodes in air (see details in the Supporting Information). In order to calibrate the distance, all curves were shifted, setting the distance of the electrodes to zero at the position of breaking the contact.

In the second set, a separate series of measurements revealed the electrical properties of single salen junctions in the non-linear regime. While performing the stretching measurements, we calculated a moving coefficient of variation (relative standard deviation) of the signal, with the window size of 100 points (last 100 measured elements). By comparing it to the preset value (CV_{lim} = 0.02), we detected a change in the stretching signal slope, and consequently, the formation of steps or slanted plateaus. When the suitable slope was detected (coefficient of variation drops below the CV_{lim}), the stretching of the junction was halted, and $I(V)$ acquisition was initiated. $I(V)$ measurements were done by performing a butterfly sweep: voltage was increased from 0 to 0.8 V, then decreased from 0.8 to −0.8 V, after that, it was again increased to 0.8 V, and we finish by returning to 0 V. In this manner, two full-range $I(V)$ curves were obtained from one single junction position. When data acquisition was finished, stretching of the junction was resumed, and after some time interval, if we were still positioned on the plateau, we could repeat the measurement. This procedure was performed until the junction was fully opened, and no molecular signal was detected. To measure again, the junction had to be fully closed to ensure that all the molecules bound to the tips were purged and that the measurement on the same molecular unit was not repeated. In other words, the junction was closed until it was around 20 G_0, and then it was all set for the next stretching cycle. Typically, to obtain high-quality data, stretching traces and $I(V)$ measurements were recorded in separate runs, due to perturbations in the signal caused by the stopping of the motor (small oscillations in position) and sweeping to the relatively high voltages (charging and electrostatic effects).

Supporting Information

Supporting Information is available from the Wiley Online Library or from the author.

Acknowledgements

S.G., A.E., A.S., and F.K. acknowledge financial support from the Helmholtz Initiative and Networking Funds via the IHRS NanoNet and the Excellence Network cfaed. S.G. acknowledges support from DCM-MatDNA (VH-KO-606, ExNet-0026, ExNet-0028) and the DFG for funding via the Center for Advancing Electronics Dresden (EXC 1056).

Open access funding enabled and organized by Projekt DEAL.

Conflict of Interest

The authors declare no conflict of interest.

Data Availability Statement

Research data are not shared.

Keywords

characterization, mechanically controllable break junction, molecular electronics, molecular tuning, salen

Received: March 11, 2021
Revised: June 29, 2021
Published online: July 30, 2021

[1] T. Sendler, K. Luka-Guth, M. Wieser, Lokamani , J. Wolf, M. Helm, S. Gemming, J. Kerbusch, E. Scheer, T. Huhn, A. Erbe, *Adv. Sci.* **2015**, *2*, 5.

[2] L. Gerhard, K. Edelmann, J. Homberg, M. Valášek, S. G. Bahoosh, M. Lukas, F. Pauly, M. Mayor, W. Wulfhekel, *Nat. Commun.* **2017**, *8*, 1.

[3] T. Esat, N. Friedrich, F. S. Tautz, R. Temirov, *Nature* **2018**, *558*, 7711.
[4] M. L. Perrin, C. J. O. Verzijl, C. A. Martin, A. J. Shaikh, R. Eelkema, J. H. van Esch, J. M. van Ruitenbeek, J. M. Thijssen, H. S. J. van der Zant, D. Dulic, *Nat. Nanotechnol.* **2013**, *8*, 4.
[5] Y. Li, M. Buerkle, G. Li, A. Rostamian, H. Wang, Z. Wang, D. R. Bowler, T. Miyazaki, L. Xiang, Y. Asai, G. Zhou, N. Tao, *Nat. Materials* **2019**, *18*, 4.
[6] L. Venkataraman, J. E. Klare, C. Nuckolls, M. S. Hybertsen, M. L. Steigerwald, *Nature* **2006**, *442*, 7105.
[7] Z. F. Liu, S. Wei, H. Yoon, O. Adak, I. Ponce, Y. Jiang, *Nano Lett.* **2014**.
[8] M. Mayor, C. von Hähnisch, H. Weber, J. Reichert, D. Beckmann, *Angew. Chem., Int. Ed.* **2002**, *41*, 1183.
[9] D. Xiang, F. Pyatkov, F. Schröper, A. Offenhäusser, Y. Zhang, D. Mayer, *Chem. – A Eur. J.* **2011**, *17*, 47.
[10] R. Davidson, O. A. Al-Owaedi, D. C. Milan, Q. Zeng, J. Tory, F. Hartl, S. J. Higgins, R. J. Nichols, C. J. Lambert, P. J. Low, *Inorganic Chem.* **2016**, *55*, 6.
[11] J. Park, A. N. Pasupathy, J. I. Goldsmith, C. Chang, Y. Yaish, J. R. Petta, M. Rinkoski, J. P. Sethna, H. D. Abruna, P. L. McEuen, D. C. Ralph, *Nature* **2002**, *417*, 6890.
[12] S. A. Getty, C. Engtrakul, L. Wang, R. Liu, S. H. Ke, H. U. Baranger, W. Yang, M. S. Fuhrer, L. R. Sita, *Phys. Rev. B* **2005**, *71*, 24.
[13] T. Albrecht, A. Guckian, J. Ulstrup, J. G. Vos, *Nano Lett.* **2005**, *5*, 7.
[14] X. Xiao, D. Brune, J. He, S. Lindsay, C. B. Gorman, N. Tao, *Chem. Phys.* **2006**, *326*, 138.
[15] M. Nielsen, K. V. Gothelf, *J. Chem. Soc., Perkin Trans.* **2001**, *1*, 2440.
[16] M. Nielsen, N. B. Larsen, K. V. Gothelf, *Langmuir* **2002**, *18*, 7.
[17] V. L. Pecoraro, W. M. Butler, *Acta Cryst.* **1986**, *42*, 9.
[18] M. El Abbassi, P. Zwick, A. Rates, D. Stefani, A. Prescimone, M. Mayor, H. S. J. van der Zant, D. Dulić, *Chem. Sci.* **2019**, *10*, 36.
[19] D. Xiang, F. Pyatkov, F. Schröper, A. Offenhäusser, Y. Zhang, D. Mayer, *Chem. – Eur. J.* **2011**, *17*, 47.
[20] K. Koyama, K. Iijima, D. Yoo, T. Mori, *RSC Adv.* **2020**, *10*, 49.
[21] R. Smit, Y. Noat, C. Untiedt, N. D. Lang, M. C. van Hemert, J. M. van Ruitenbeek, *Nature* **2002**, *419*, 6910.
[22] J. M. Van Ruitenbeek, A. Alvarez, I. Pineyro, C. Grahmann, P. Joyez, M. H. Devoret, D. Esteve, C. Urbina, *Rev. Sci. Instrum.* **1996**, *67*, 1.
[23] K. Luka Guth, S. Hambsch, A. Bloch, P. Ehrenreich, B. M. Briechle, F. Kilibarda, T. Sendler, D. Sysoiev, T. Huhn, A. Erbe, E. Scheer, *Beilstein J. Nanotechnol.* **2016**, *7*, 1.
[24] A. Magyarkuti, N. Balogh, Z. Balogh, L. Venkataraman, A. Halbritter, *Nanoscale* **2020**, *12*, 15.
[25] L. A. Zotti, T. Kirchner, J.-C. Cuevas, F. Pauly, T. Huhn, E. Scheer, A. Erbe, *Small* **2010**, *6*, 14.
[26] P. Gehring, J. M. Thijssen, H. S. van der Zant, *Nat. Rev. Phy.* **2019**, *1*, 6.
[27] S. Datta, *Electronic Transport in Mesoscopic Systems*, Cambridge Studies in Semiconductor Physics and Microelectronic Engineering. Cambridge University Press, Cambridge **1995**.
[28] W. Hong, D. Z. Manrique, P. Moreno-Garcia, M. Gulcur, A. Mishchenko, C. J. Lambert, M. R. Bryce, T. Wandlowski, *J. Am Chem. Soc.* **2012**, *134*, 4.
[29] C. Li, I. Pobelov, T. Wandlowski, A. Bagrets, A. Arnold, F. Evers, *J. Am Chem. Soc.* **2008**, *130*, 1.
[30] K. V. Gothelf, A. Thomsen, M. Nielsen, E. Cló, R. S. Brown, *J. Am Chem. Soc.* **2004**, *126*, 4.
[31] D. C. Milan, O. A. Al-Owaedi, M.-C. Oerthel, S. Marqués-González, R. J. Brooke, M. R. Bryce, P. Cea, J. Ferrer, S. J. Higgins, C. J. Lambert, P. J. Low, D. Z. Manrique, S. Martin, R. J. Nichols, W. Schwarzacher, V. M. García-Suárez, *J. Phys. Chem. C* **2016**, *120*, 29.
[32] V. Fatemi, M. Kamenetska, J. B. Neaton, L. Venkataraman, *Nano Lett.* **2011**, *11*, 5.
[33] L. Kankate, A. Turchanin, A. Gölzhäuser, *Langmuir* **2009**, *25*, 18.
[34] J. Ponce, C. R. Arroyo, S. Tatay, R. Frisenda, P. Gavina, D. Aravena, E. Ruiz, H. S. J. van der Zant, E. Coronado, *J. Am Chem. Soc.* **2014**, *136*, 23.